

Circularly permuted green fluorescent proteins engineered to sense Ca^{2+} and their application to imaging of subcellular Ca^{2+} dynamics

Atsushi Miyawaki,^{*1} Takeharu Nagai,^{*1,*2} Satoshi Shimozone,^{*1,*3}

Takashi Fukano,^{*1} and Hideaki Mizuno^{*1}

^{*1}Laboratory for Cell Function Dynamics, BSI, RIKEN

^{*2}Japan Science and Technology Corporation

^{*3}School of Pharmaceutical Sciences, University of Tokyo

To visualize Ca^{2+} -dependent protein-protein interactions in living cells by fluorescence readouts, we utilized a circularly permuted green fluorescent protein (cpGFP), in which the amino and carboxyl portions had been interchanged and reconnected by a short spacer between the original termini. The cpGFP was fused to calmodulin and its target peptide, M13. The chimeric protein, which we have named "pericam", was fluorescent and its spectral properties changed reversibly with the amount of Ca^{2+} , probably due to the interaction between calmodulin and M13, leading to an alteration of the environment surrounding the chromophore. Three types of pericam were obtained by mutating several amino acids adjacent to the chromophore. Of these, "flash-pericam" became brighter with Ca^{2+} , while "inverse-pericam" dimmed. On the other hand, "ratiometric-pericam" had an excitation wavelength that changed in a Ca^{2+} -dependent manner. All the pericams expressed in HeLa cells were able to monitor free Ca^{2+} dynamics, such as Ca^{2+} oscillations in the cytosol and the nucleus. To obtain confocal images of Ca^{2+} using ratiometric-pericam, we established a system in which two laser beams (excitation 408 and 488 nm) are alternated on every scanning line under the control of two acousto-optic tunable filters. We visualized the dynamic changes of Ca^{2+} concentrations in highly motile mitochondria of HeLa cells. Our new confocal imaging system will expand the range of potential applications of ratiometric-pericam and other dual-excitation ratiometric indicators.

Introduction

Wild-type GFP (WT-GFP) has a bimodal absorption spectrum with two peak maxima at 395 and 475 nm, corresponding to the protonated (neutral) and deprotonated (anionic) states of the chromophore, respectively.¹⁾ The ionization state is modulated by a hydrogen bond network that comprises an intricate network of polar interactions between the chromophore and several surrounding amino acids. The chromophore of most GFP variants titrates with single pKa values, indicating that the internal proton equilibrium is disrupted by external pH. One variant, the yellow fluorescent protein (YFP), has a T203Y substitution responsible for the red-shift emission at 528 nm. Ormö *et al.* predicted that the tyrosine introduced at position 203 is involved in a π -stacking interaction with the chromophore.²⁾ This idea was later confirmed by X-ray crystallography.³⁾ In this review, we describe how we have developed new fluorescent indicator proteins for Ca^{2+} based on GFP, for monitoring concentrations of free Ca^{2+} in subcellular structures, such as mitochondria.

Circularly permuted yellow fluorescent protein

Within the rigid "β-can" structure of GFP variants, Baird *et al.* found a site that would tolerate circular permutations, where two portions of the polypeptide are flipped around the central site.⁴⁾ With obvious clefts in the β-can, the chromophore of circularly permuted GFPs (cpGFPs) seems to

be more accessible to protons from outside the protein. The cpGFPs may be used to convert changes in the interaction between two protein domains into a change in the electrostatic potential of the chromophore, in other words, to transduce information about the interaction into a fluorescent signal. A less pH-sensitive YFP variant, EYFP.1,⁵⁾ was subjected to circular permutation. The original N- and C-termini were fused via a pentapeptide linker GGSGG and Y145 and N144 were made the new N- and C-termini, respectively. The resulting chimeric protein is called cpEYFP.1

Construction of pericams

M13 is the calmodulin (CaM)-binding peptide of myosin light chain kinase. We first made a construct, in which cpEYFP.1 was fused to the C-terminus of M13 through a tripeptide linker SAG, and through a GTG linker to the N-terminus of the E104Q CaM mutant (Fig. 1). We utilized a variant of CaM, in which the conserved bidentate glutamate at position 104 in the third Ca^{2+} binding loop was changed to glutamine.⁶⁾ Since the N-terminus of CaM and the C-terminus of M13 were rather far apart (58Å when the complex was formed), the β-barrel of cpEYFP.1 might be considerably twisted. However, this radically designed chimeric protein was fluorescent and, as we hoped, showed Ca^{2+} sensitivity. The protein, having a circularly permuted EYFP.1 and a CaM, was named "pericam".⁷⁾ The CaM and M13 projecting from cpEYFP.1 also reminded us of the bill of a pelican.

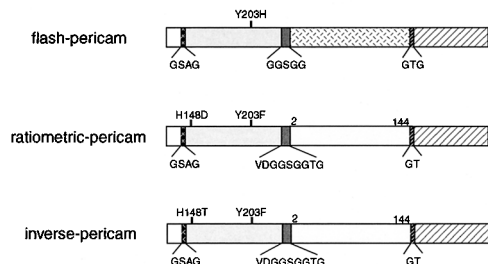
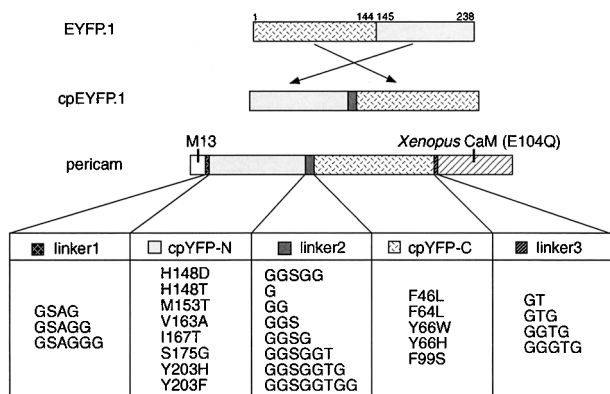


Fig. 1. Strategy for the construction of pericams. On the basis of pericam, intensive optimization of linkers and amino acids (listed in a table) was performed to create flash-pericam, ratiometric-pericam, and inverse-pericam. The optimized amino acid sequences of linkers and amino acid substitutions for the three pericams are shown below and above the bars, respectively.

When excited at 485 nm, Ca^{2+} -bound pericam showed an emission peak at 520 nm, three times brighter than Ca^{2+} -free pericam (data not shown).

Flash-pericam

To obtain pericams with a larger dynamic range, we optimized several amino acids involved in the proton coordinating network. Substitution of His203 for Tyr improved the dynamic range significantly. The new pericam, called “flash-pericam” (Fig. 1), exhibited an 8-fold increase in fluorescence in the presence of Ca^{2+} (Fig. 2D), suggesting it could be used as a single wavelength indicator of the concentration of free Ca^{2+} ($[\text{Ca}^{2+}]$). In the absence of Ca^{2+} , flash-pericam exhibited an absorbance spectrum similar to that of cpEYFP.1 (Fig. 2A, broken line). Upon saturation with Ca^{2+} , the 490-nm absorbance peak increased at the expense of the 400-nm peak (Fig. 2A, solid line), indicating that the association of Ca^{2+} -CaM with the M13 peptide deprotonated the chromophore, resulting in a leftward shift of the pH-titration curve (Fig. 2G). Note that the Ca^{2+} -bound flash-pericam with the ionized chromophore at pH 9 was about twice as bright as the Ca^{2+} -free one (at pH > 10). Therefore, the interaction between CaM and M13 might have direct steric effects on the chromophore that are separate from the pH effect, and changed its ionization state or reduced its out-of-plane distortions in a way that enhanced radiationless decay. The latter possibility is likely, because Ca^{2+} binding to flash-pericam increased the quantum yield several fold as well as the molar extinction coefficient around 490 nm (data not shown). Fig. 2G shows that Ca^{2+} -bound flash-pericam was alkaline-quenched (pH > 10), suggesting that the incomplete β -can structure collapsed.

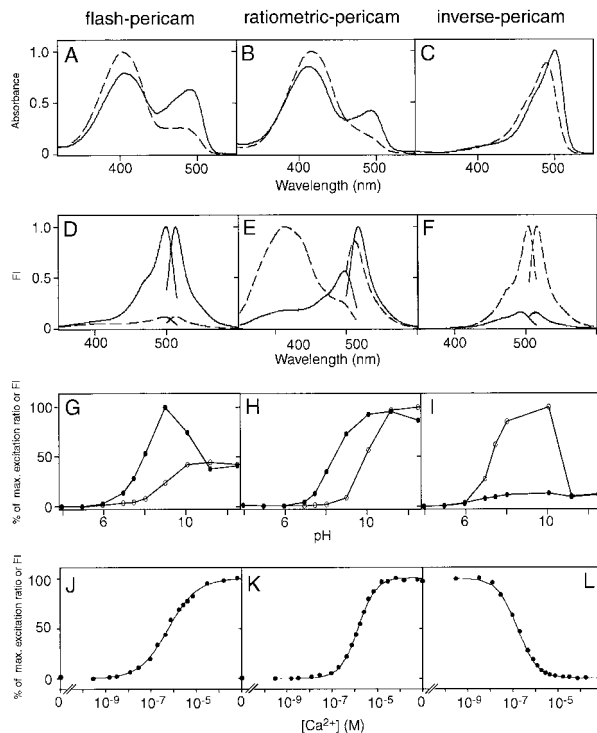


Fig. 2. *In vitro* properties of flash-pericam (A, D, G, and J), ratiometric-pericam (B, E, H, and K), and inverse-pericam (C, F, I, and L). Absorbance (A–C) and fluorescence excitation and emission (D–F) spectra of pericams. (A–F) The spectra and data points were obtained in the presence (solid line) or absence (broken line) of Ca^{2+} . (G–I) pH dependence of normalized amplitudes of the 514-nm emission peak (G) and of the 516-nm emission peak (I) as well as the excitation ratio of 495/410 (H) in the presence (closed circles) and absence (open circles) of Ca^{2+} . (J–L) Ca^{2+} titration curves of pericams. FI, fluorescence intensity.

Ratiometric-pericam

Most YFPs have a tyrosine or a histidine at position 203 and contain non-fluorescent protonated species that absorb at around 400 nm.¹⁾ Similarly, fluorescence was hardly detectable when flash-pericam was excited at around 400 nm. On the other hand, replacing the amino acid at position 203 in YFP with phenylalanine made the protonated species fluorescent and allowed it to, upon excitation at 400 nm, give rise to a predominant emission peak at 455 nm,⁸⁾ suggesting that proton transfer in the excited state is inhibited. The 455-nm emission indicates the existence of protonated excited state species. Hoping to create a ratiometric Ca^{2+} indicator, we introduced Phe203 in flash-pericam. Again, the linkers and several amino acids proved critical for the optimization of protein folding and Ca^{2+} sensitivity. After numerous constructs were tested, “ratiometric-pericam” was derived from flash-pericam by introducing the mutations H203F, H148D, and F46L; deleting a glycine before CaM; and replacing the GGSGG linker between the original N- and C-termini with VDGGSGGTG (Fig. 1). As was seen with flash-pericam, Ca^{2+} binding promoted ionization of the chromophore in ratiometric-pericam. Therefore, it exhibited a Ca^{2+} -dependent change in the absorbance spectrum, similar to the case of flash-pericam (Fig. 2B), and the pH-titration curve was shifted leftwards in the presence of Ca^{2+} (Fig. 2H). In contrast to flash-pericam, however, ratiometric-pericam

had a bimodal excitation spectrum with peaks at 415 and 494 nm (Fig. 2E), and the relative intensities of green fluorescence (511–517 nm) emitted when excited with 494- and 415-nm light were changed by about tenfold between the Ca^{2+} -saturated and the Ca^{2+} -free forms (Fig. 2E). The excitation ratio (494/415) showed a monophasic Ca^{2+} dependence with an apparent dissociation constant (K_d) of 1.7 μM and a Hill constant of 1.1 (Fig. 2K).

Inverse-pericam

During the semi-random mutagenesis of ratiometric-pericam, we found an interesting protein with the substitution D148T, which emitted green fluorescence (513–515 nm) when excited at 500 nm but decreased to 15% in the presence of Ca^{2+} (Fig. 2F), essentially the opposite of the case of flash-pericam. Thus, the protein was named “inverse-pericam” (Fig. 1). One possibility is that the binding of Ca^{2+} to inverse-pericam may have promoted protonation of the chromophore. However, the following results indicate that this was not the case. At pH 7.4, Ca^{2+} only red-shifted the peak of the absorbance spectrum from 490 to 503 nm, with no change in the tiny hump around 400 nm (Fig. 2C); Ca^{2+} binding thus appears not to have affected the protonation state of the chromophore. Also, both the Ca^{2+} -bound and Ca^{2+} -free inverse-pericams were pH-titrated with similar pKas (Fig. 2I). In fact, we found that the quantum yield decreased with Ca^{2+} binding (data not shown). These findings suggest that the change in fluorescence intensity is mostly due to a direct effect of the Ca^{2+} -related structural change on the chromophore.

$[\text{Ca}^{2+}]_i$ imaging in HeLa cells expressing pericams

When each pericam was expressed in HeLa cells, the fluorescence was uniformly distributed throughout the cytosolic and nuclear compartments but excluded from the nucleoli, as expected for a 44 kDa protein, which can pass through the nuclear pores. Thus, the pericams can report intracellular $[\text{Ca}^{2+}]_i$ s. Figures 3A, 3B and 3C show receptor-stimulated $[\text{Ca}^{2+}]_i$ oscillations in single HeLa cells expressing flash-pericam, ratiometric-pericam and inverse-pericam, respectively. In each case, the response began with a large spike, became sinusoidal, then converted into transient spikes with gradually declining frequency.

Compared with single-wavelength indicators (flash-pericam and inverse-pericam), ratiometric-pericam permits quantitative Ca^{2+} imaging that can cancel out artifacts produced by indicator concentration and cell thickness or movement. In the presence of Ca^{2+} ionophore, the application of a high concentration (5 mM) of extracellular Ca^{2+} , then BAPTA-AM and EGTA gave the maximum and minimum ratios (R_{max} and R_{min} , respectively) for an *in situ* calibration (Fig. 3B, top). The amplitude of the first spike was about 3 μM , while that of the subsequent spikes was below 1 μM . The relatively weak Ca^{2+} affinity allows for a more precise quantification of spike amplitude than fura-2, the popular dual-excitation ratiometric Ca^{2+} indicator.

The time course of inverse-pericam (Fig. 3C) seems to be a symmetric image of that of the flash-pericam (Fig. 3A). However, inverse-pericam showed more sustained $[\text{Ca}^{2+}]_i$ increases (Fig. 3C). This is consistent with the finding that inverse-pericam had a higher affinity for Ca^{2+} than flash-

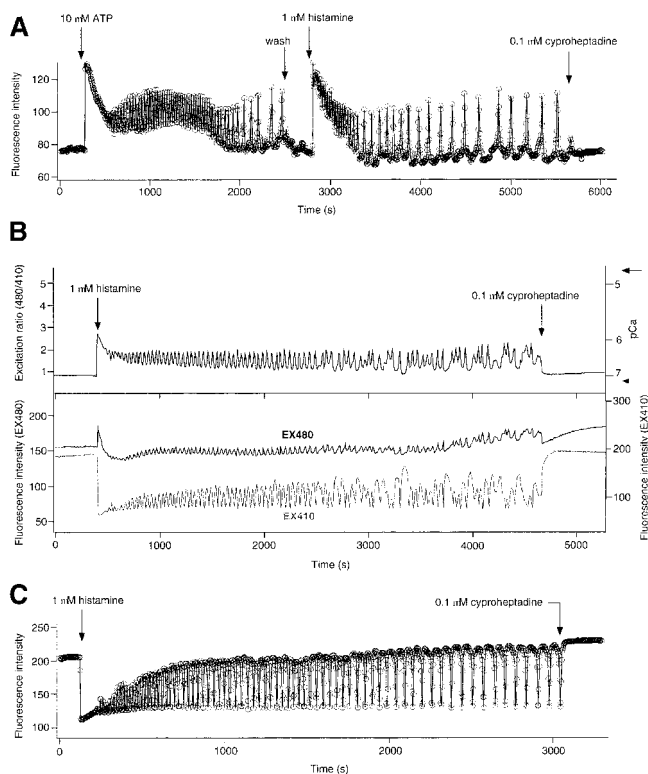


Fig. 3. Typical $[\text{Ca}^{2+}]_i$ transients and oscillations induced by receptor stimulations in HeLa cells expressing flash-pericam (A), ratiometric-pericam (B), inverse-pericam (C). The sampling interval was 3–5 s. (B, Upper) Excitation ratios, 480–410 nm. The right-hand ordinate calibrates $[\text{Ca}^{2+}]_i$ in pCa with R_{max} and R_{min} indicated by an arrow and an arrowhead, respectively. (Lower) 480 nm (black line, left-hand scale) and 410 nm (gray line, right-hand scale) excitations.

pericam; their K_d values were 0.2 and 0.7 μM , respectively (Figs. 2J and 2L). One feature of inverse-pericam is that its Ca^{2+} -free form has a high molar extinction coefficient and a quantum yield at pH 7.4, which are almost comparable to those of enhanced GFP.²⁾ Thus, despite the unusual characteristics of dimming with Ca^{2+} , the use of inverse-pericam permits Ca^{2+} imaging with a satisfactory signal-to-noise ratio.

Confocal imaging of Ca^{2+} using ratiometric-pericam

Dual-excitation ratiometric dyes, such as ratiometric-pericam, permit quantitative Ca^{2+} measurements by minimizing the effects of several artifacts that are unrelated to changes in the concentration of free Ca^{2+} ($[\text{Ca}^{2+}]_i$), such as uneven loading or partitioning of dye within the cell, or varying cell thickness. Usually the excitation wavelength is alternated using a rotating wheel containing two bandpass filters or a high-speed grating monochromator. Use of the monochromator can increase the rate at which the ratio measurement is conducted to about 10 Hz. These measurements are performed using conventional microscopy, which is suitable for producing the excitation peaks. However, monitoring of the changes in $[\text{Ca}^{2+}]_i$ is often severely limited by the poor spatio-temporal resolution of conventional wide-field microscopy. To obtain more reliable information on changes in

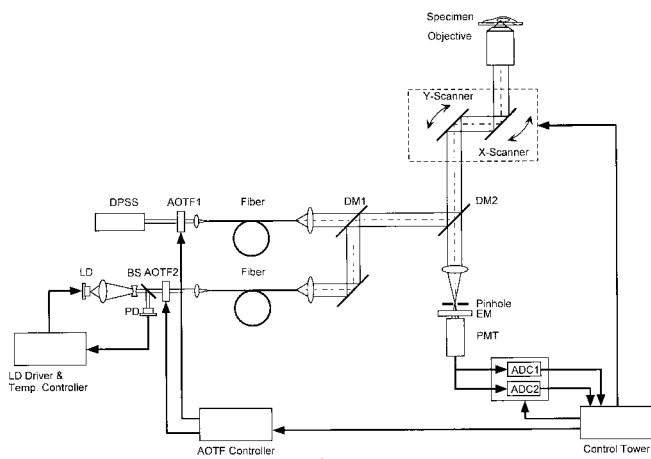


Fig. 4. Schematic diagram of the laser-scanning confocal microscopy system for fast dual-excitation ratiometric imaging. DPSS, diode-pumped solid-state laser; LD, laser diode; PD, photodiode; BS, beam splitter; DM, dichroic mirror; EM, emission filter; PMT, photomultiplier tube; and ADC, analog-to-digital converter.

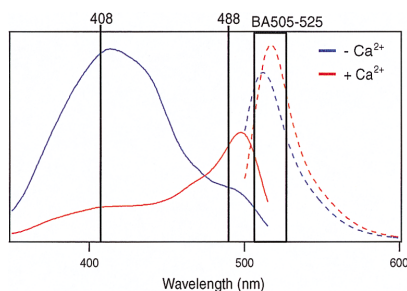


Fig. 5. Fluorescence excitation (solid lines) and emission (dashed lines) spectra of ratiometric-pericam in the presence (red) and absence (blue) of Ca^{2+} . Two laser lines, 408 (laser diode) and 488 nm (diode-pumped solid state), are indicated by vertical lines. The wavelengths that pass through the emission filter BA505–525 are shown by a box.

subcellular $[\text{Ca}^{2+}]_m$, we needed to increase the z-axis resolution and the speed of production and collection of the ratios of the excitation peaks.

Here we describe a modified laser-scanning confocal microscopy (LSCM) system for ratiometric-pericam.⁹⁾ Fast exchange between two laser beams was achieved using acousto-optic tunable filters (AOTFs) (Fig. 4). Samples were scanned on each line sequentially by a violet laser diode (408 nm) and a diode-pumped solid-state laser (488 nm). In this way, the ratios of the excitation peaks can be obtained at frequencies of up to 200 Hz. These lasers were chosen for their efficiency of excitation of ratiometric-pericam (Fig. 5), and for their stability, which is important for dual-excitation ratiometric measurements.

Calcium transients in motile mitochondria

The cationic probe rhod2 has been widely used to measure $[\text{Ca}^{2+}]_m$ in mitochondria ($[\text{Ca}^{2+}]_m$), but its targeting specificity relies on the negative membrane potential of this or-

ganelle. The Ca^{2+} -sensitive photoprotein aequorin, on the other hand, can be specifically targeted to mitochondria and has been used to monitor mitochondrial Ca^{2+} dynamics. However, aequorin requires the incorporation of coelenterazine, is irreversibly consumed by Ca^{2+} , and is very difficult to image because of its weak luminescence. To overcome these limitations, we used the ratiometric-pericam selectively targeted to mitochondria in HeLa cells. At first, changes in $[\text{Ca}^{2+}]_m$ were monitored by alternating the excitation wavelength automatically with wide-field conventional microscopy. In these studies, the rate of acquisition of the excitation ratio was about 10 Hz, which was identical to the frame rate. Despite this high data collection rate, the $[\text{Ca}^{2+}]_m$ measurements were often adversely affected by the active motion of mitochondria, especially at higher temperatures. Therefore, using our LSCM technique, we attempted to increase the speed of the alteration of excitation wavelengths so that it was higher than the velocity of mitochondria. With this method, the frame rate was 5 Hz and the rate of ratio acquisition was 200 Hz. Although the frame rate did not allow us to fully follow the rapid movement of mitochondria, the high rate of ratio acquisition minimized the time lag between the two measurements used to make each ratio signal. We believe that this method of imaging $[\text{Ca}^{2+}]_m$ effectively corrects for movement of mitochondria laterally or into and out of the optical section. After the application of histamine, spots of $[\text{Ca}^{2+}]_m$ increase within a single mitochondrion were identifiable (Fig. 6A) and the global increase in $[\text{Ca}^{2+}]_m$ was found to occur relatively slowly (Fig. 6B).

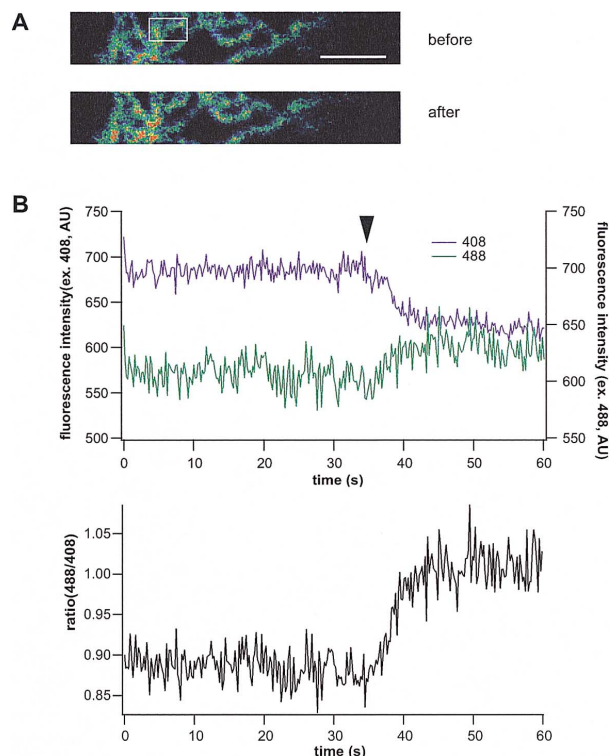


Fig. 6. Confocal and dual-excitation imaging of $[\text{Ca}^{2+}]_m$ using ratiometric-pericam-mt. (A) Ratio images before and after application of $10 \mu\text{M}$ histamine. (B) Time course of the averaged fluorescence signals from the white box in (A) with excitation (ex) at 488 nm (green) and 408 nm (violet) (top) and the ratio (bottom). The arrowhead indicates the time when histamine was applied. AU, arbitrary units.

References

- 1) R. Y. Tsien: *Annu. Rev. Biochem.* **67**, 509 (1998).
- 2) M. Ormö, A. B. Cubitt, K. Kallio, L. A. Gross, R. Y. Tsien, and S. J. Remington: *Science* **273**, 1392 (1996).
- 3) R. M. Wachter, M. A. Elsliger, K. Kallio, G. T. Hanson, and S. J. Remington: *Structure (London)* **6**, 1267 (1998).
- 4) G. S. Baird, D. A. Zacharias, and R. Y. Tsien: *Proc. Natl. Acad. Sci. USA* **96**, 11241 (1999).
- 5) A. Miyawaki, O. Griesbeck, R. Heim, and R. Y. Tsien: *Proc. Natl. Acad. Sci. USA* **96**, 2135 (1999).
- 6) A. Miyawaki, J. Llopis, R. Heim, J. M. McCaffery, J. A. Adams, M. Ikura, and R. Y. Tsien: *Nature* **388**, 882 (1997).
- 7) T. Nagai, A. Sawano, E.S. Park, and A. Miyawaki: *Proc. Natl. Acad. Sci. USA* **98**, 3197 (2001).
- 8) R. M. Dickson, A. B. Cubitt, R. Y. Tsien, and W. E. Moerner: *Nature* **388**, 355 (1997).
- 9) S. Shimozono, T. Fukano, T. Nagai, Y. Kirino, H. Mizuno, and A. Miyawaki: *Science's stke (Web)* (2002).